AN ABSTRACT OF THE THESIS OF

Ahmed A. El Tayyan for the degree of Master of Science in Physics presented on June 9 ,1988 .

Title : Measurements of Atmospheric Sodium by Direct Absorption of Sunlight.

Abstract approved: Redacted for Privacy
C. E. Fairchild

The atmospheric sodium daytime abundance was measured for Corvallis, Oregon, using direct absorption of sunlight by atmospheric sodium atoms, as observed with an optical waveguide spectrum analyzer. The disadvantage of the spectrum analyzer is that it can't resolve the sodium D-lines (Its resolving power is 0.5 nm, which is approximately the same as the wavelength separation of the sodium D lines). The data analysis is based on a model developed specifically for atomic absorption of resonance radiation. In this model only the first order approximation was considered, and any further development of the model needs to consider the higher order terms. A daytime variation in the atmospheric sodium abundance having a maximum at around noon was observed. Also, a day-to-day variation in the atmospheric sodium abundance was observed. The results obtained in this experiment are consistent with previous results obtained at Madison, Wisconsin, by measuring the atmospheric transmission of sunlight at the Na D2 wavelength using a high resolution multiple Fabry-Perot spectrometer.

MEASUREMENTS OF ATMOSPHERIC SODIUM

ABUNDANCE BY DIRECT ABSORPTION OF SUNLIGHT

BY

AHMED ASAD EL TAYYAN

A Thesis

submitted to

Oregon State University

in partial fulfillment of
the requirement for the
degree of

Master of Science

Completed June 9, 1988

Commencement June 1989

APPROVED:

Redacted for Privacy

Professor of Physics in charge of major

Redacted for Privacy

Chairman of the Department of Physics

Redacted for Privacy

Dean of Graduate School

Date thesis is presented June 9, 1988

Typed by Ahmed El Tayyan for Ahmed El Tayyan

AKNOWLEDGEMENTS

I would like to thank Dr. C . E. Fairchild for all the inspiration he has given me, not just as a thesis advisor, but through all my time here at O.S.U. I would also like to thank Dr. K. Krane for his support and kindness. Also I would like to thank Dr. Carl Kocher for being a good understanding teacher and for being a member of my thesis committee.

I would like to thank all my instructors here at O.S.U. for the effort they put into their classes.

I would also like to thank all my classmates who suffered and struggled along side with me through our years of study.

TABLE OF CONTENTS

LIST OF FIGURES

MEASUREMENTS OF ATMOSPHERIC SODIUM ABUNDANCE BY DIRECT ABSORPTION OF SUNLIGHT

Chapter 1

Introduction to Atmospheric Sodium

1.1. Background

The existence of free sodium atoms in the Earth's upper atmosphere was first proposed in the late 1930's as a result of detecting strong radiation in the resonance lines of sodium in the twilight sky (1). It was found by many investigators (2) that the intensity of λ = 589.0 nm and 589.6 nm is greatly enhanced at twilight. This suggested that there is resonance scattering of the solar radiation by the free sodium atoms(2):

$$Na\ (3S) + \gamma\ \{\ 589.0 \text{ or } 589.6 \text{ nm}\} \dashrightarrow Na\ (3P)\ ,$$

followed by

$$Na\ (3P) \dashrightarrow Na\ (3S) + \gamma\ \{\ 589.0 \text{ or } 589.6 \text{ nm}\}$$

Another explanation by Vegard (3) is that the excited atoms are released in photodissociation by sunlight of sodium compounds. By studying the absorption of the D doublet using a sodium cell kept at different temperatures, Bricard and Kastler (2) were able to show that the temperature of the emitting atoms in the atmosphere must be about 240 ± 50 K. This result favors the resonance scattering theory because the fragments of a molecule which suffers photodissociation have considerable initial kinetic energy.

The intensity of the morning twilight flash first increases as the

Sun approaches the horizon because the radiation can reach more and more sodium atoms without attenuation in the lower atmosphere. Then it reaches a plateau, and finally, it drops as a result of the absorption of solar radiation by sodium atoms (4,5). A similar behaviour occurs in the evening, except that it is reversed in time. The observations of many workers in either the Northern hemisphere (6) or the Southern hemisphere (7) showed that the intensity is greater in winter than in summer, and occasional fluctuations about the mean occur.

Many suggestions have been proposed to explain the existence of sodium compounds in the upper atmosphere(1,8,9). Unfortunately none of these suggestions is definite. Does the existance of sodium in the upper atmosphere have a terrestrial origin, or does it come to the atmosphere from outer space?. Some of the suggestions are:

a. Volcanic dust containing sodium compounds enters the atmosphere.

b. Sodium salt may be carried out from ocean sprays by ascending currents of air into the upper atmosphere.

c. The Sun may be the source and the sodium comes with the solar corpuscular streams which produce auroral and magnetic disturbance phenomena.

d. The sodium may exist in interplanetary space, and sweeps into the earth's atmosphere while the earth moves through this space.

e. Meteors may be the source of atmospheric sodium (See chapter 1, Sec. 3.A) .

f. Debris from thermonuclear bomb tests may add some contribution to atmospheric sodium (10).

The following discussion was exerpted from Mitra(1), and it represents how workers used to think about atmospheric sodium in the past. Chapman (11) in 1937 proposed a cyclic process in which the free sodium atoms form sodium compounds (NaO and / or NaH) which dissociate yielding excited sodium atoms due to collision with oxygen atoms. Regarding the formation of sodium compounds the reactions may be imagined to be the following:

$$Na + O_2 + M \rightarrow NaO_2 + M$$

$$NaO_2 + H \rightarrow NaH + O_2$$

$$NaO_2 + O \rightarrow NaO + O_2$$

$$NaO_3 \rightarrow NaO + O_2$$

$$Na + OH + M \rightarrow NaOH + M$$

where M is any free neutral particle. The reactions which lead to dissociation of the sodium compounds may be imagined to be:

$$NaO + O \rightarrow Na^* + O_2$$

$$NaH + O \rightarrow Na^* + OH \quad .$$

Another reaction suggested by Rowland and Mikide (12) is the following:

$$NaOH + \gamma\ (uv) \rightarrow Na + OH \qquad (\lambda \leqslant 346\ nm)$$

It is possible that Na+ ions undergo radiative recombination

$$e + Na+ \rightarrow Na + \gamma$$

The neutral sodium atoms are excited to a higher energy level of the S, P ,D or F states, and then drop to the 2P states which emit the D-lines. Another radiative recombination which may occur is

$NaOH + \gamma \rightleftharpoons Na + OH$, but most probably NaOH formations are stabilized by collision [See (1) above.] because typical radiative lifetimes are long compared with the lifetime of collision complexes.

As is explained in the following section, the abundance of free sodium atoms is an important aspect of atmospheric sodium studies. Many workers investigated whether there is a daytime enhancement in sodium abundance or not. The study of the direct absorption of sunlight by the atmospheric sodium layer (13,14,15,16,17) showed no clear diurnal variations. However, the work of Partowmah and Roestler (18) on the direct absorption of sunlight by atmospheric sodium showed some diurnal variations (This method will be explained in Sec.3). Also, Kirchhoff (19) showed theoretically that there is diurnal variation in atmospheric sodium (See Figure 1.1.). The seasonal variation of atmospheric sodium abundance has been reported (18,7) with a maximum in winter and a minimum in summer.

1.2. Reasons for studying atmospheric Na

By studying atmospheric sodium important information can be obtained about the atmospheric constituents and characteristics such as:

A. Methane & OH

The release of methane from rice paddies, the rumen of cattle, swamps, and other anaerobic biological processes increases its concentration in the upper atmosphere (20)(in the Northern Hemisphere more than Southern Hemisphere).

The increase of the tropospheric CH_4 causes an increase in the sratospheric water vapour, forming polar clouds which may increase the depletion of the ozone layer. Also, CH_4 makes a contribution to the

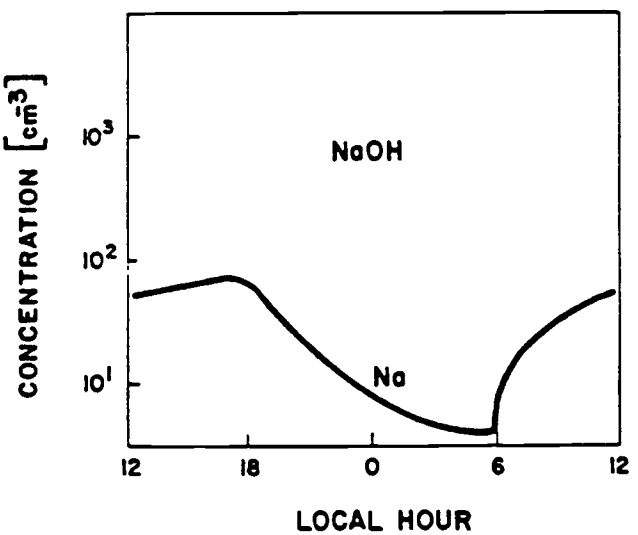

Figure 1.1 . Diurnal variation of atmospheric sodium concentration at 80 Km as calculated by Kirchhoff (19). The sodium concentration increases diuring the day until it reaches maximum around 6 p.m. , then it starts to drop until it reaches minimum around 6 a.m., this curve does not agree with our results.

atmospheric greenhouse effect by causing infrared absorption in the wavelength regions which are not strongly absorbed by atmospheric O_3, H_2O and CO_2. Measurments in different seasons showed different structures in the latitudinal concentration gradient of CH4 (20). These changes in the gradient structure may be related to the seasonal nature of the OH attack on CH_4, i.e., CH_4 is removed by reaction with OH according to the following cycle (21):

$$OH + CH_4 \rightarrow CH_3 + H_2O$$

$$CH_3 + O_2 \ (+M) \rightarrow CH_3O_2 \ (+M)$$

$$CH_3O_2 + NO \rightarrow CH_3O + NO_2$$

$$CH_3O + O_2 \rightarrow HCHO + HO_2$$

$$HCHO + \gamma \rightarrow H_2 + CO$$

$$HCHO + \gamma \longrightarrow H + H\,O$$

$$OH + HCHO \rightarrow H_2O + HCO$$

$$H + O_2 + M \rightarrow HO_2 + M$$

$$HCO + O_2 \rightarrow HO_2 + CO$$

$$HO_2 + NO \rightarrow OH + NO_2$$

$$HO_2 + O_3 \rightarrow OH + 2\,O_2$$

This shows the importance of studying atmospheric OH .

It was found (22) that NaOH is one of the basic atmospheric sodium species, and it may be the dominant one at around the peak of the neutral sodium layer which is at 94 Km (23). Some of the reactions that lead to the formation of NaOH can be described as follows(24):

$$Na + HO_2 \rightarrow NaOH + O$$

$$NaO_2 + H \rightarrow NaOH + O$$

Also, $Na + OH + M \rightarrow NaOH + M$.

Probably a small contribution of OH compared with the last reaction can be obtained from the following reaction:

$$Na + OH \dashrightarrow NaOH + \gamma \quad .$$

A reaction that leads to the formation of the OH molecule can be imagined as follows (25):

$$NaOH + Cl \dashrightarrow NaCl + OH$$

Also, $NaOH + \gamma\ (uv) \dashrightarrow Na + OH \quad (\lambda \leqslant 346\ nm)$.

Thus, studying atmospheric sodium may lead to information about the atmospheric OH, which tends to react with other atmospheric constituents and is difficult to detect directly, and which, in turn, may yield information about CH_4.

B. Determination of ozone density:

Additional chemical reactions of atmospheric sodium can be described as follows (26,27)

$$Na + O_3 \dashrightarrow NaO + O_2$$

$$NaO + O \dashrightarrow Na^* + O_2$$

These reactions lead to a model to calculate the mesospheric ozone density at a height of 88 Km (28).

C. Studying the mesospheric winds:

Observations of the atmospheric sodium layer using a laser radar technique proved that this layer exhibits a wave-like structure (29,30,31). The study of the Na density variation leads to information about the motion inside the sodium layer (29).

D. Studying the eddy diffusion coefficient:

The eddy diffusion coefficient is responsible for transporting the sodium between a source and sink (7). Thus,

studying the sodium distribution provides a method to deduce information about the eddy diffusion coefficient (32).

1.3. Review of some atmospheric Na studies

A. The sodium budget:

Lamb and Benson (33) found that the major constituents of meteoroides by weight are: Al(1.7%), Fe(11.5%), Ca(1.5%), Si(20%), Na(2%), Mg(12.5%), Ni(1.5%). Other metals like Ti ,Mn ,and Cr have been observed in micro-meteorites collected in the stratosphere.

Hughes (34) estimated the total meteoroid flux to the earth to be about 1.6×10^{10} g yr^{-1}. About 70% of the incoming meteoroid mass blow away (35). This gives a sodium influx of about $1.2 * 10^{23}$ atoms s^{-1}, which yields a flux of about 2.3×10^{4} atoms cm^{-2} s^{-1} of Na when averaged over the surface of the earth.

Using the value for the flux of sodium into the stratosphere, the concentration of sodium in the bottom of the stratosphere, has been calculated (33) as a function of diffusion into the troposphere. The calculation assumed that the sodium is conserved and at steady state (i.e, the input flux at the top of the stratosphere is equal to the flux out across the tropopause.). The sodium concentration due to all sodium species at 20 km was estimated to be $5.1 * 10^{6}$ cm^{-3}. Also the column density for all sodium species between 20 and 85 km (where sodium atoms are produced from meteoroid blowing away) was calculated (33) according to the following equation:

$$\Sigma C_h = \int_{20}^{85} C_h \, dh = H \times C_{20} \int_{0}^{65} \exp(-h/H) \, dh$$

where H is the scale hight, C_h is the sodium density at height h and C_{20} is the sodium density at height 20 km. This equation gave a column density of 3.5×10^{12} Na cm^{-2} of all forms of sodium constitutents.

B. Absorption studies of daytime sodium abundance:

By measuring the transmission of sunlight at the Na D_2 wavelength using a high resolution multiple Fabry-Perot spectrometer Partowmah and Roestler (University of Wisconson, Madison) determined (18) that there is a daytime variation in atmospheric sodium abundance with a maximum at noon. These investigators also observed a seasonal variation in atmospheric sodium abundance having a maximum in winter. Their spectrometer is a Pepsios spectrometer (15,23,36) with three Fabry-Perot etalons in a common pressure chamber with a resolution limit of about 0.060 cm^{-1} corresponding to $\Delta \lambda \simeq 0.002$ nm. Noting that the Doppler breadth Δ_D is defined as $\Delta v_D = [2(2 R \ln 2)^{1/2}] [v/c] [T/M]^{1/2}$ (See Chapter 2, Sec.4), the Doppler breadth of the atmospheric Na D_2 line is $\Delta \lambda_D \simeq 0.004$ nm. Spectral profiles of the bottom of the sodium D_2 line in sunlight were recorded by linear scans at different times of the day. The scans were about 0.7 cm^{-1} long (corresponding to $\Delta \lambda \simeq 0.025$ nm $\simeq 6 \Delta \lambda_D$) centered at the bottom of the sodium D_2 line. Each scan took 2.5 to 3.5 min, and data points were recorded in 2.0 s intervals. The profile of sunlight through a hot sodium cell was taken periodically every few scans as a reference for adjacent traces.

The seasonal abundance variation, Figure 1.2, shows a maximum

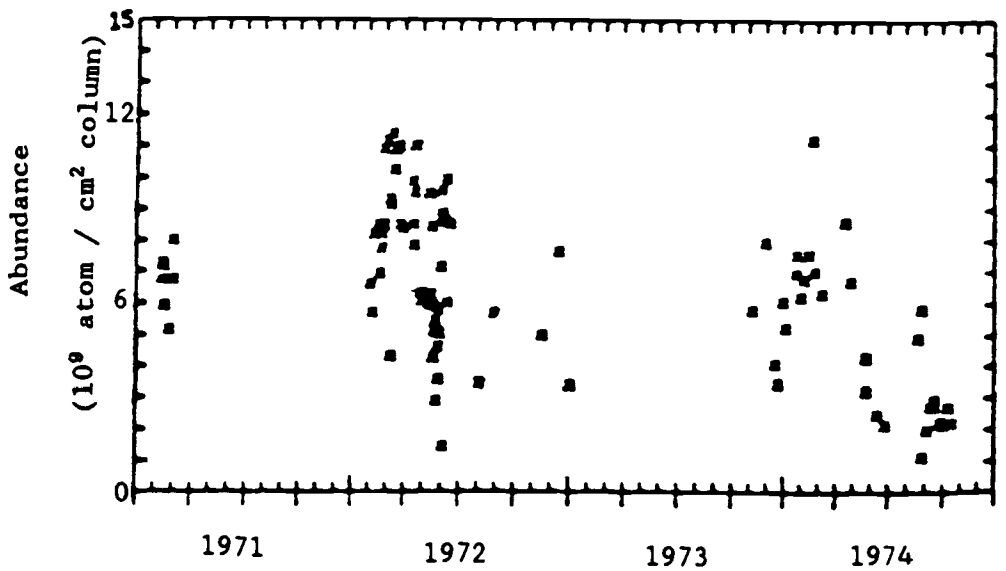

Figgure 1.2. Daily averages of the Na abundance from Feb. 1971 to Oct. 1974 . It shows that the abundance is minimum in summer and maximum in winter. These data were taken at Madison Wisconsin(18).

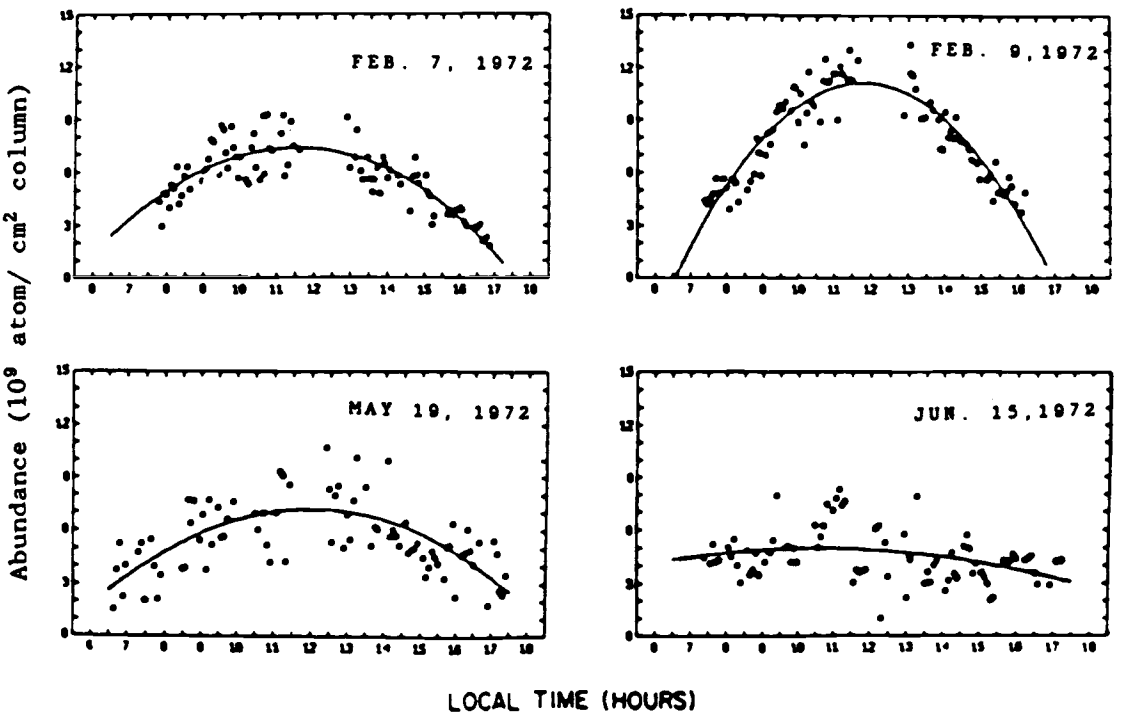

Figgure 1.3. Diurnal variation of sodium abundance on four representative days . It shows that a daytime enhancement seems to occur around the time of the local noon. These data were taken at Madison, Wisconsin (18).

around February-March (7.7×10^9 atom / cm^2), and minimum around July (2.9×10^9 atom / cm^2). The diurnal variation of sodium abundance on four days shows a maximum at noon, as shown in Figure 1.3.

Consultation of the local climatological data showed an indication that the atmospheric sodium abundance may be correlated with the Earth's albedo. It was found that the average abundance increases when there is a fresh covering of snow on the ground (presumably giving a high albedo) while the daily abundance was less than average on the days in which the snow cover was old (presumably resulting in lower albedo).

C. The laser radar technique:

The laser radar technique provides a suitable method for calculating the nighttime density of atmospheric sodium as a function of height. The basic procedure of this technique is exciting the atmospheric neutral atomic sodium population with short duration and small bandwidth laser light pulses. Then, resonantly back scattered photons are collected by a large mirror, which focusses the light onto a photomultiplier. The signal produced in the lidar apparatus can be expressed as (7,37)

$$C(h) = n(h)\ \rho\ K\ T^2\ /\ h^2 \quad ,$$

where C(h) is the number of photons detected per pulse which are received during a small time interval centered at $t \simeq 2h\ /c$, n(h) is the density of the scattered molecules at height h, ρ is the Rayleigh backscattering function per molecule, and T is the atmospheric transmission. For each laser pulse, Rayleigh scattering from the stratosphere is detected as a temporal event occuring just prior to

resonant scattering from mesospheric sodium, therefore; we can form the ratio of these two signals to obtain

$$Na(h_1) = \{ C(h_1) \cdot D(h_2) \rho_R \ h_1^2 \} / \{ C(h_2) \rho_{Na} \ h_2^2 \}$$

where $Na(h_1)$ is the sodium density at height h_1, $D(h_2)$ is the molecular density at height h_2, and ρ_{Na}, ρ_R are the effective resonant back scattering function for sodium atoms and the average Rayleigh back scattering function, respectively.

Figure 1.4. shows several profiles of the sodium layer averaged over different time periods. Figure 1.5 shows the abundance of atmospheric sodium. It shows a day to day variation in the abundance; and it confirms that the abundance is minimum in Summer, in agrement with the Partowmah results (18).

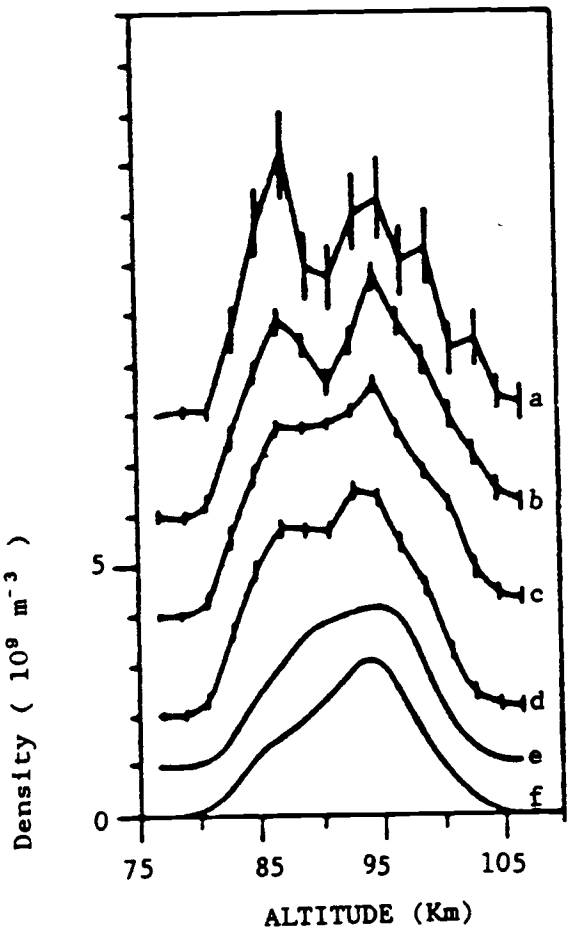

Figure 1.4 .Several profiles of atmospheric sodium layer for different times: (a) three minutes, (b) one hour , (c) seven hours, (d) July 30 to July 31, 1975 ,(e) the month of July and (f) is 1975 average. Noting that the zero level has been shifted for clarity. These data were taken at Sao Paulo, Brazil (7).

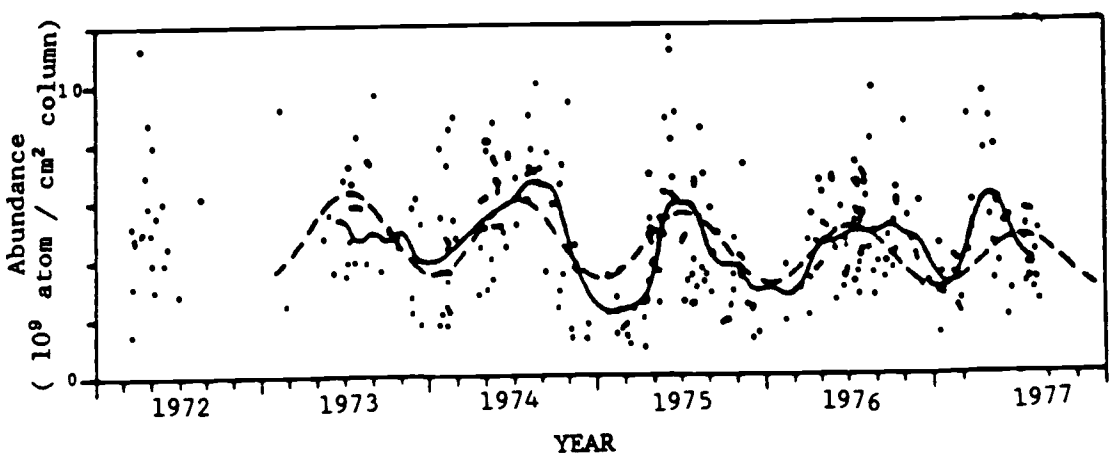

Figure 1.5 . The average nightly Na abundance of over several years. The solid curve coresponds to a three month running mean, and the broken curve is the best fit sinusoid. Abundance is a minimum in summer. These data were taken at Sao Paulo, Brazil (7).

Chapter 2

Modeling Absorption of Sunlight by Atmospheric Sodium

2.1. Introduction

The Sun is a star which consists of 64 per cent hydrogen , 32 per cent helium, and about 4 per cent other elements-including almost every known stable element. The total energy emitted from the Sun as a result of thermonuclear reactions in the interior is approximately equal to that radiated by a black body with a temperature equal to 5750 K (38).

The photosphere is the visible disc of the sun with a diameter equal to 1.3920×10^6 Km. It is not uniformaly bright, but it contains some dark spots. Also its intensity decreases as we move towards the periphery. It is covered with a small rapidly changing cellular structure with diameters of about 1000 Km.

The chromosphere is the lower part of the region above the photosphere, between radii of 1×10^4 to 2×10^4 Km with an average temperature of about 4500 K.

The solar corona is the region surmounting the chromosphere. Its temperature increases gradually with altitude until it reaches a maximum value at about 5×10^4 Km height. This maximum value of temperature was estimated to be of the order of 2×10^6 K (2) (See Figure 2.1). The solar corona is composed mainly of ionized hydrogen in addition to a small amount of a fully ionized helium atoms (alpha particles). It also contain some other elements such as

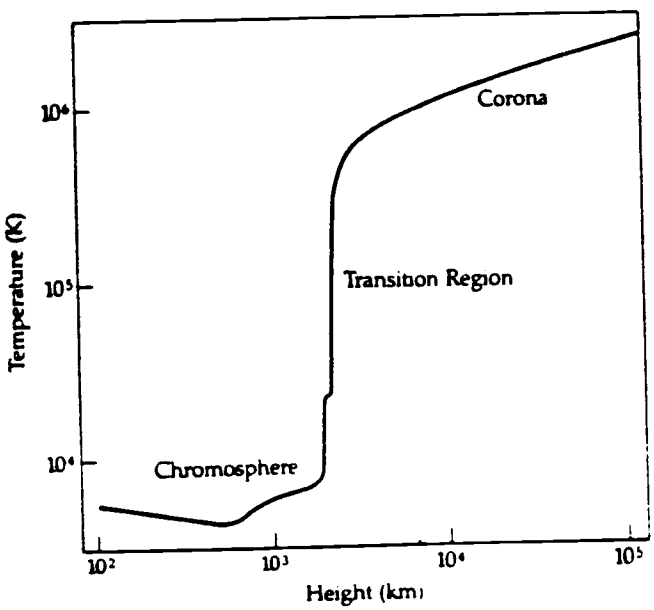

Figure 2.1 .The temperature structure in the chromosphere and corona (42).

oxygen and carbon which are almost completely ionized. Also, it contains heavier elements such as iron, calcium, nickel and argon which are highly but incompletely ionized .

The radiation received from the Sun is similar to that of a black body. In the solar spectrum the wavelength corresponding to maximum energy is about 500 nm for a surface temperature of 5750 K. The solar spectrum consists of a large number of dark lines called Fraunhofer lines. These lines were studied by Fraunhofer in 1814. These absorption lines are observed throughout the visible spectrum. Fraunhofer measured the wavelength of many of these lines and found that they occupied the same positions as the bright lines emitted by different gases and vapours.

According to Kirchhoff's law of radiation, any material at a lower temperature will absorb the radiations of those wavelengths which it will emit when excited in an electrical discharge. Thus, the Fraunhofer lines are the absorption lines of relatively cooler gases and vapours present in the sun's atmosphere and the earth's atmosphere.

The most prominent Fraunhofer lines are denoted by letters of the alphabet. Some of these lines, with their wavelengths and the elements responsible for their absorption are given below:

line	element	wavelength in nm
A	Atmospheric oxygen	759.4
B	Atmospheric oxygen	686.7
C	Hydrogen	656.3
D1	Sodium	589.6

D2	Sodium	589.0
F	Hydrogen	486.1
G1	Hydrogen	434.1
H	Calcium	496.9
K	Calcium	393.4

During a solar eclipse, the Fraunhofer lines can be seen in emission from the chromosphere (39). This fact, together with the temperature distribution of the thermosphere (See Figure 2.1), leads to the development of a line absorption model for absorption of sunlight by atmospheric sodium. The early parts of this model are developed in Section 4 of this chapter.

The primary properties of the Earth's atmosphere are density, pressure, composition, temperature and motion. It was believed in the past that the temperature of the atmosphere decreases indefinitely to the top of the atmosphere. This raised the idea that the atmosphere has a height of around 50 Km (38).

Later, de Bort (38), using registering thermometers carried on kites, discovered that the temperature ceases to decrease at a height of about 10 Km. At this height the temperature gradient either falls to a lower value, or is reversed.

The troposphere is the lower atmospheric region of changing weather, and the stratosphere is the upper region where T is almost uniform. The region between them is called the tropopause. Other subregions have been identified, and other names have been proposed, such as stratopause, mesopause, mesosphere and thermosphere.

2.2 Sodium and the resonance radiation phenomenon

It was known (40) that if sodium vapour at some pressure in a heated test-tube is illuminated from a gas flame (yellow flame) containing a NaCl solution, a yellow fluorescence will be seen emerging from the tube from the point at which the exciting light enters. Spectroscopic investigation of this fluorescence shows that it contains the two sodium D-lines. This phenomenon is called resonance fluorescence, which is defined as follows: The atoms in the normal state absorb light of certain frequencies, and subsequently re-emit light of the same frequencies.

The quantum theory easily explains resonance radiation. If a continuous spectrum of light of wavelength ranging between 200 and 600 nm is passed through a quartz cell containing sodium vapour, the sodium atoms in the normal state $3^2 S_{1/2}$ will absorb the D-lines and undergo a transition to the $3^2 P_{1/2}$ or $3^2 P_{3/2}$ states. Later the excited atoms in the 3^2 P states will undergo transitions to the $3^2 S_{1/2}$ state, emitting the D-lines as fluorescence.

2.3. Simple model

The following model is used here to determine the effective thickness of the atmospheric sodium layer at different zenith angles. It is based on the Van Rhijn method used to determine the height of a luminescent layer (1).

Let h_1 be the vertical height (zenith angle z = 0) of the bottom of the sodium layer, as shown in Figure 2.2. The ray ob makes an angle z with the ray od. Let the length of the ray ob be L_1.

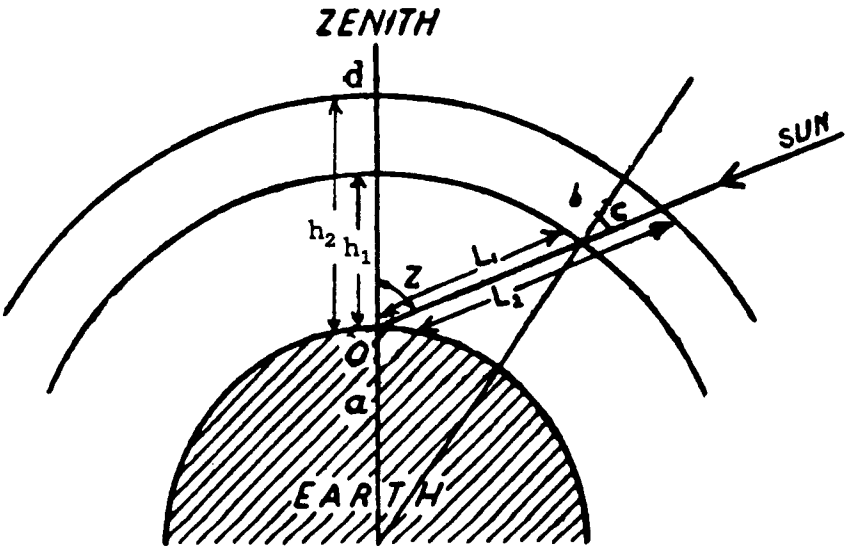

Figure 2.2 . Simple Model to calculate the effective width of the atmospheric sodium layer.

If the layer is assumed to be horizontal and flat (neglecting the curvature of the earth), then

$$L_1 = h_1 \sec z \quad .$$

If the curvature of the layer is taken into account, then approximately,

$$L_1 = h_1 \sec c \quad ,$$

where c is given by

$$\sin c = [\, a /(a + h_1)] \sin z \quad .$$

In the later equation, a is the radius of the earth.

Repeating the calculation for h_2 and L_2 we find

$$L_2 = h_2 \sec c$$

The distance that the solar ray has to travel at zenith angle z inside the atmospheric sodium layer is given by

$$X = L_2 - L_1$$

2.4. Model for calculating the average density of atmospheric neutral sodium

If a beam of light of a continuous spectrum be sent through an absorbing cell containing a monatomic gas, the absorption coefficient k(v) is defined by the equation

$$I(v) = I_0(v) \exp[-k(v)\, X] \qquad (1)$$

where $I_0(v)$ is the spectral irradiance (per unit bandwidth) of the incident radiation, I(v) is the spectral irradiance of the transmitted radiation, and X is the thickness of the absorbing cell.

Now consider a parallel beam of light of frequency between v and v + dv and spectral irradiance I(v) passing through a layer of

atoms between X and X+dX. Let N be the number of atoms per unit volume in the layer, let δN_v be the number of atoms capable of absorbing the frequency range between v and v + dv, and let N^* be the number of excited atoms, of which δN_v^* are capable of emitting this frequency range. If we neglect the effect of spontaneous re-emission, because it takes place in all directions, then the decrease in the intensity of the beam is given by

$$- d[I(v)\ \delta v\ ] = \delta N_v\ \ dX\ hv\ \ B_{12}\ [I(v)\ /4\pi\ ] - \delta N^*_v\ \ dX\ hv\ \ B_{21}\ \ [I(v)\ /4\pi\ ] \qquad (2)$$

where B_{12} and B_{21} are Einstein coefficients, which are defined as:

B_{12} . I(v) = probability per unit time that the atoms in state 1 exposed to isotropic radiation of spectral irradiance I(v) and frequency ranging between v and v +dv, will absorb a quantum hv and pass to state 2.

B_{21} I(v) = probability per second that the atom will undergo transition from state 2 to state 1 when it exposed to radiation of spectral irradiance I(v) and frequency ranging between v and v + dv, emitting radiation in the same direction as the direction of the stimulating radiation.

$I(v)\ /4\pi$ is the spectral irradiance of the equivalent isotropic radiation for which B_{12} and B_{21} are defined.

Equation (2) can be rewritten as

$$-1/I(v)\ [dI(v)\ /dX]\ \delta\ v = (h\ v/4\pi)\ (B_{12}\ \ \delta\ N_v - B_{21}\ \delta\ N_v^*) \qquad (3)$$

comparing equations (1) and (3), we find that

$$K(v)\ \delta v = (h\ v\ /4\pi)\ \ (B_{12}\ \ \ \delta\ N_v\ - B_{21}\ \ \delta\ N_v^*) \qquad (4)$$

Now, integrating equation (4) over the whole absorption line and

neglecting the small variation of v throughout the line,

$$\int K(v)\ dv = (h\ v_0\ /4\pi)\ (B_{12}\ N - B_{21}\ N^*) \qquad (5)$$

where v_0 is the frequency of the center of the line.

Einstein showed that

$$A_{21}\ /\ B_{12} = 2\ h\ v^3\ g_1\ /c^2\ g_2\ , \qquad (6)$$

and

$$B_{21}\ /\ B_{12} = g_1/g_2 \qquad (7)$$

where A_{21} is the propability per second that the atom in state 2 will emit h v sponteneously and pass to state 1. So, $A_{21} = 1\ /\tau$ where τ is the lifetime of the atom. Also, g_1 and g_2 are the statistical weights of the normal and excited states respectively.

Using equations (6) and (7), equation (5) can be rewritten

$$\int K(v)\ dv = (\lambda_0^2\ N\ g_2/8\pi\ \tau\ g_1)\ (1-\ g_1\ N^*\ /g_2\ N) \qquad (8)$$

For sodium atoms in the Earth's atmosphere, $g_1\ N^*/g_2\ N \ll 1$ (The excitation of atoms due to the beam of light.). Therefore, equation (8) takes the form

$$\int K(v)\ dv = \lambda_0^2\ g_2\ N\ /\ 8\pi\ g_1\ \tau \qquad (9)$$

Before finding an expression for the absorption coefficient K(v) it is a good idea to mention the processes that contribute to the formation of the absorption line of a gas. These processes are:

A. Natural broadening(1)

An excited molecule remains in its state until a downward transition is induced by an electromagnetic field;i.e., spontaneous decay takes place. The width of the observed spectral line is given by

$$\alpha_N = \Delta\ v\ /\ 2 \simeq 1\ /\ 4\ \tau) \quad ,$$

where τ is the natural life time.

B. Doppler broadening

The frequency bandwidth of a gas increases due to the random thermal motion of its atoms. It results in a gaussian spectrum (See appendix).

C. Lorantzian broadening

If the radiating atom suffers a collision, it loses energy causing the duration of emission to be shortened and the frequency bandwidth to increase.

D. Stark effect

It is due to collisions with electrons and ions.

E. Holtsmark broadening

It is due to collision with other absorbing atoms of the same kind.

It is known (40) that, when the thermal motion of the atoms is taken into account, and the natural damping is neglected, then the absorption coefficient of a gas is given by

$$K(v) = k_0 \exp-[2(v - v_0)(\ln 2)^{1/2}/\Delta_D]^2 \qquad (10)$$

where Δv_D is the Doppler breadth, defined as:

$$\Delta v_D = [\, 2(2 R \ln 2)^{1/2} / c \,]\, v_0 \, (T/M)^{1/2} \qquad (11)$$

where R is the universal gas constant, T is the absolute temperature, M is the molecular weight, and v_0 is the frequency at the center of the line.

Integrating equation (10) gives

$$\int_0^\infty K(v)\, dv = \int_0^\infty ko \exp -[2(v - v_0) (\ln 2)^{1/2} / \Delta v_D]^2$$

$$= 1 / 2 \, (\pi / \ln 2)^{1/2} \, k_0 \, \Delta v_D \qquad (12)$$

Comparison between equations (9) and (12) yields

$$k_0 = 2 / \Delta v_D \quad (\ln 2 / \pi)^{1/2} (\lambda_0^2 / 8\pi) (g_2 N / g_1 \tau) . \qquad (13)$$

If $k_0 = K_0 N$, then

$$K_0 = 2 / \Delta v_D \quad (\ln 2/\pi)^{1/2} \quad (\lambda_0^2 / 8\pi) \quad (g_2 / g_1 \tau) \quad . \qquad (14)$$

Hence, equation (12) becomes

$$\int_0^\infty K(v)\, dv = \int_0^\infty K_0 N \exp -[2(v - v_0)(\ln 2)^{1/2} / \Delta v_D]^2 \, dv$$

$$= \int_0^\infty N\, k(v)\, dv$$

$$= N (\pi / \ln 2)^{1/2} K_0 \Delta v_D / 2 \qquad (15)$$

If the solar radiation in a frequency range dv at v passes through a layer of thickness X containing N sodium atoms per unit volume at some time on its way to Earth, then equation (1) becomes

$$I(N,v) = I_0(v) \quad \exp -[K(N,v) \quad X] \qquad (16)$$

at a later time, due to the rotation of the earth on its axis, the solar radiation will travel a distance $X' = X + \Delta X$ and the number of sodium atoms becomes $N' = N + \Delta N$, where ΔN can be either positive or negative.

$$I(N',v) = I_0(v) \quad \exp -[K(N',v) \quad X'] \qquad (17)$$

Integrating equations (16) and (17), then dividing them and setting $\int_0^\infty I(N,v)\, dv = I$ and $\int_0^\infty I(N',v)\, dv = I'$, we obtain

$$I / I' = \int_0^\infty I_0(v) \quad \exp -(K(N,v) \quad X)\, dv \; /$$

$$\int_0^\infty I_0(v) \exp -[K(N',v)\, X'] \quad . \qquad (18)$$

since atmospheric absorption by sodium atoms is always small, we can expand the integrands in the denominator and numerator in Taylor series, and keep only the first two terms, which yields

$$I/ I' = \int_0^\infty I_0(v) \, [1-K(N,v) \quad X]\, dv \; /$$

$$\int_0^\infty I_0(v) \, [1-K(N',v) \quad X']\, dv \qquad (19)$$

Now, using the notations in equation (15), we find that

$$K(N,v) = K(v)\ N$$

$$K(N',v) = K(v)\ N' \quad . \tag{20}$$

Hence, equation (19) becomes:

$$I / I' = \int_0^\infty Io(v)\ [1 - N\ K(v)\ X]\ dv\ /$$

$$\int_0^\infty Io(v)\ [1 - N'\ K(v)\ X'\ ]\ dv \tag{21}$$

Taking $\int_0^\infty Io(v)\ dv = Io$ the last equation becomes

$$I / I' = \{I_0 - N\ X \int_0^\infty I_0(v)\ K(v)\ dv\}\ /$$

$$\{I_0 - N'\ X' \int_0^\infty I_0(v)\ K(v)\ dv\ \}$$

$$= [1 - (N\ X / I_0) \int_0^\infty I_0(v)\ K(v)\ dv\ ]\ /$$

$$[1 - \{(N + \Delta N)(X + \Delta X) / Io\} \int_0^\infty I_0(v)\ K(v)\ dv] \tag{22}$$

The denominator of equation (22) has the form $1/(1 - y)$. This form has the expansion $1/(1 - y) = \sum_{n=0}^{\infty} y^n \qquad y < 1$

Hence, expanding the denominator of equation (22), and taking only the first two terms, we get

$$I / I' = \{\ 1 - (N\ X / I_0) \int_0^\infty I_0(v)\ K(v)\ dv\ \}/$$

$$\{\ 1 - [(\ N + \Delta\ N\ )(\ X + \Delta\ X\ )/\ I_0\ ] \int_0^\infty I_0(v)\ K(v)\ dv\ \}$$

$$I / I' = \{[\ 1 - N\ X \int_0^\infty I_0(v)\ K(v)\ dv\ ]/[\int_0^\infty I_0(v)\ dv\ ]\}$$

$$\{\ 1 + [(N + \Delta N)(X + \Delta X) \int_0^\infty I_0(v)\ K(v)\ dv]/[\int_0^\infty Iov\ dv]\}$$

$$I / I' \simeq 1 + \Delta N(X + \Delta X) + N\ \Delta X]$$

$$[\int_0^\infty I_0(v)\ K(v)\ dv\ ]/[\int_0^\infty I_0(v)\ dv\ ] \quad .$$

Since $\log (1 + \epsilon) = \epsilon$ for small ϵ, the last equation can be rewritten as

$$\log[I / I'] = [\Delta N\ (X + \Delta X) + N\ \Delta X]$$

$$[\int_0^\infty I_0(v)\ K(v)\ dv]/[\int_0^\infty I_0(v)\ dv\ ] \tag{23}$$

Noting that $I_0(v)$ can be written as

$$I_0(v) = C_v \exp -[2(v - v_0)\ (\ln 2)^{1/2} / \Delta v_{Dsun}\ ]^2 \tag{24}$$

$$\log[I / I'] = [\ \Delta N\ (X + \Delta X) + N\ \Delta X]\ \ A/B \qquad (25)$$

where A and B are

$$A = Ko\ \{ \int_{o}^{\infty} \exp -[2(v - v_0)(\ln 2)^{1/2} / \Delta v_{Dearth}]^2$$

$$\exp - [2(v - v_0)(\ln 2)^{1/2} / \Delta v_{Dsun}]^2 \}$$

$$B = \int_{o}^{\infty} \exp - [2(v - v_0)(\ln 2)^{1/2} / \Delta v_{Dsun}]^2$$

When applied to the data of the present experiment the atomic resonance absorption model described above yields consistent results. Further justification for the use of this model is given in the following chapter, and the procedure for its application to the data obtained here is described in Chapter 4.

Chapter 3

Experimental Procedure for the Determination of the Atmospheric Sodium Abundance

3.1. Introduction:

The atmospheric daily average abundance of sodium was measured for Corvallis, Oregon by direct absorption of sunlight by atmospheric sodium atoms using an optical waveguide spectrum analyzer with a resolution limit 0.5 nm. Measurements were taken on the roof of Weniger Hall by mounting a solar tracker on the roof, and mounting the input end of an optical fiber bundle on the tracker. The detection of direct sunlight only was ensured by mounting an internally blackend stainless steel collimator tube of 3 mm diameter and 30.5 cm length on the solar tracker in the tracking position and inserting the input end of the optical fiber bundle into the receiving end of the collimator. The optical fiber bundle then served to guide sunlight into entrance slit of the spectrum analyzer which was located inside a rooftop laboratory.

3.2. Experimental procedure

A. The apparatus

The apparatus of this experiment consists of three main devices as shown in Figure 3.1. These devices are:

1. **Solar tracker:**

The solar tracker tracks the sun during the day time allowing for successive measurments under the same condition of alignment.

2. The OPTICAL WAVEGUIDE SPECTRUM ANALYZER:

It is connected to the solar tracker through an optical fiber cable. It performs five distinct functions:

a. Light dispersion: A grating (1200 lines/ mm) disperses the polychromatic light into smaller wavelength intervals. The grating angle associated with the wavelength of light on the detector is obtained using the grating equation (45):

$$\sin (w - \theta/2) = - k n \lambda / (2 \cos \theta/2)$$

where K is the order.

n is the number of rulings on the grating per unit length.

λ is the wavelength.

w is the angle of incidence.

θ is the angle between the enterance port, grating, and the detector.

b. Light detection: by rotating the grating the dispersed light passes through the exit slit and into the detector allowing the grating / detector combination to scan the intensity components of the dispersed spectra. The spectrum analyzer has two photodiode detectors, silicon and germanium; the silicon photodiode detector was used for these measurements.

c. Light generation: by means of an internal source (20 watt Ge 788 Tungsten-Halogen lamp operating at 6 VDC) that generates light for the spectrophotometric applications and spectroradiometric calculations. Two lenses are used to focus the lamp radiation onto the input port adapters.

d. Light chopping: This function causes the light to be

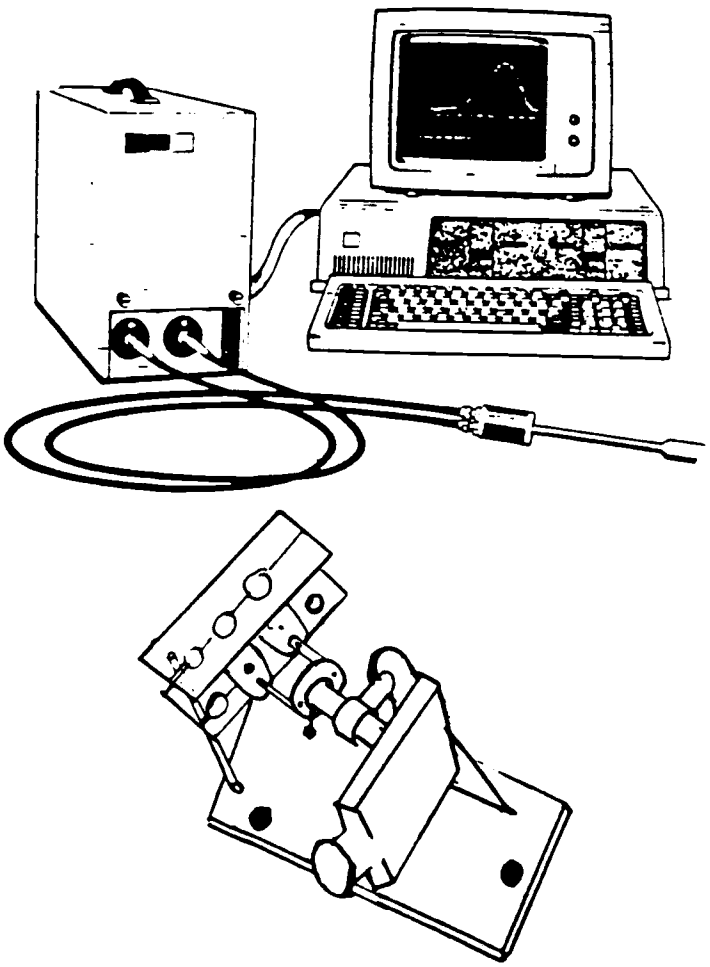

Figure 3.1. The optical waveguide spectrum analyzer, computer and solar tracker.

blocked from entering the monochromator housing every half sampling period. Specifying the sample dwell cycle provides a waiting period before the data for each wavelength is sampled, which enables the grating to stabilize before the data collection begins.

e. The input/output function: It is an interface to the computer which provides weighting, timing and formatting to the computer and storage and conversion of commands from the computer.

f. Resolving power of the spectrum analyzer: The resolving power available is determined by the minimum level of usable aplical throughput. In the spectrum analyzer used here, The minimum usable width of entrance and exit slits is 1 mm, approximately; and, the instrumental resolution of 0.5 nm is governed by these slit widths. With an instrumental resolution of 0.5 nm there is no way we could observe Na D line absorption from a continuum (broad bandwidth) emission spectrum. The Doppler width of the atmospheric Na D line absorption profile is $\Delta\lambda_D$ = 0.004 nm approximately. Even if absorption was "complete" varied from zero to the Na D line absorption, the corresponding change in photocurrent measured in the spectrum analyzer would be only two percent, which is too small to be detected.

3. The computer:

IBM personal computer. By means of a program it controls the operations of the spectrum analyzer. Data are stored in two arrays (see Figure 3.2), one of which contains the reference data and the other holds the sample data. These data can be stored on a disk to be used at later time. It performs many other operations such as calibrating the spectrum analyser and controlling all the

operations performed by the spectrum analyzer.

B. Experimental procedure:

Scans of the solar spectrum in the vicinity of the sodium D-lines were obtained during the daytime using the optical waveguide spectrum analyzer. The procedure for obtaining the solar spectrum was fairly straightforward. It can be described by the following steps:

1. Boot up the computer, turn on the spectrum analyzer, and run the spectrum analyser program for wavelength calibration of the instrument.

2. Collect a reference spectrum and store it.

(Steps 1 and 2 are not necessary every day, but the reference spectrum must be recalled before taking any new data.).

3. Adjust the solar tracker by pointing it toward the Sun .

4. Collect the data (solar spectrum between 580.0 and 595.0 nm) and store it in a file and/or obtain a graph of the spectrum(See Figure 3.3).

5. Repeat step 4 every hour throughout the day.

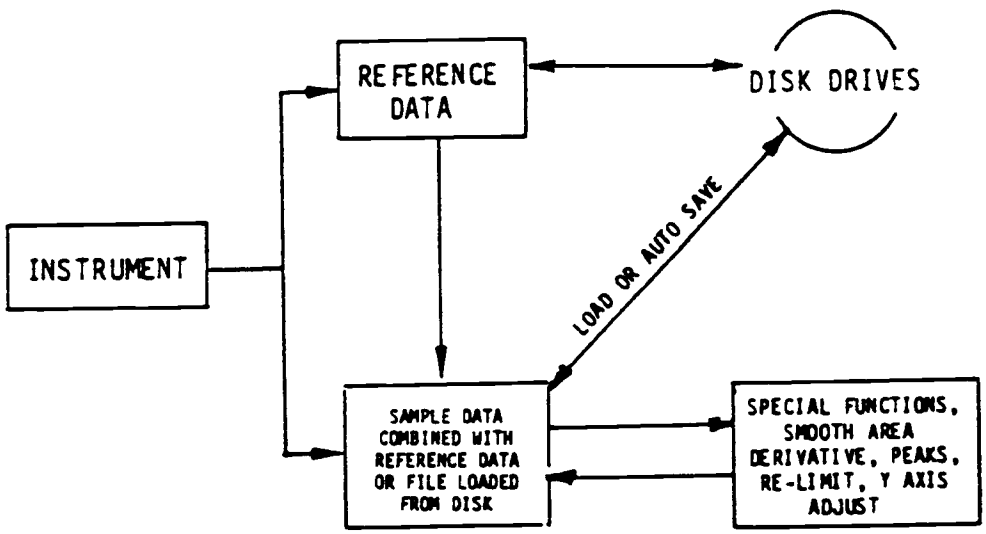

Figure 3.2 .Schematic diagram shows the processes of collecting and storing data using the optical waveguide spectrum analyzer.

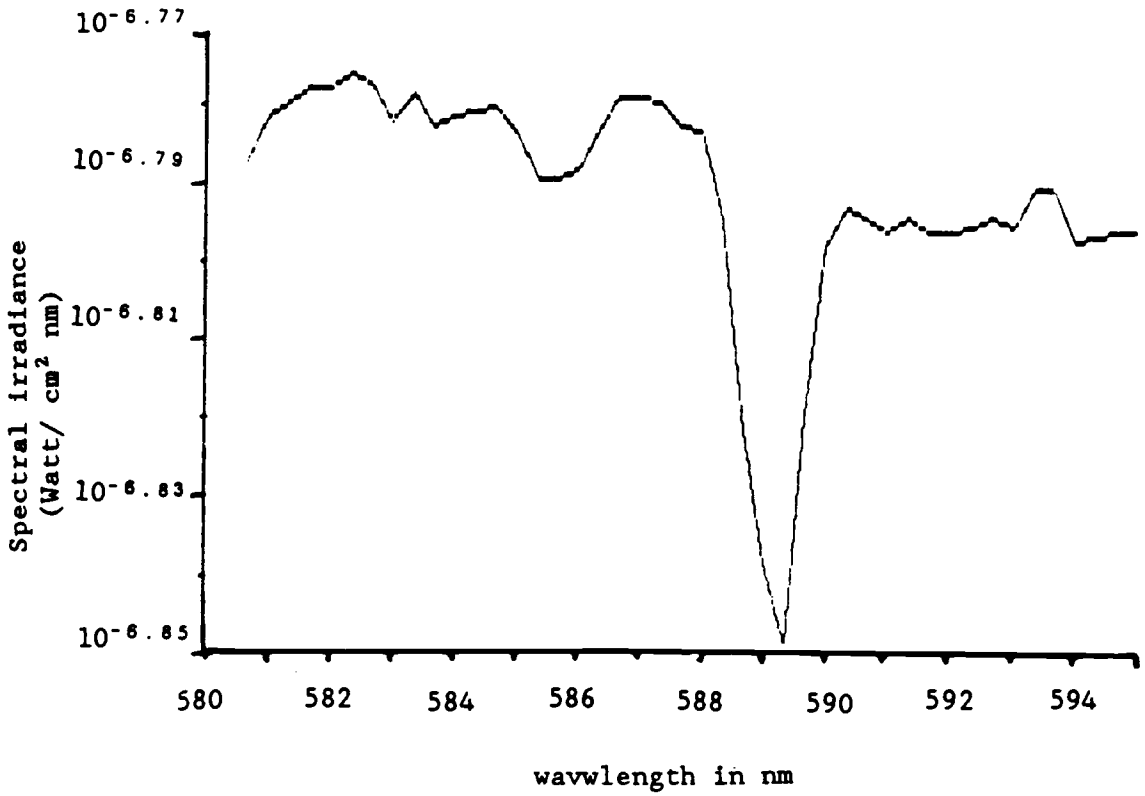

Figure 3.3 .The solar spectrum profile in the region between 580.0 and 598.0 nm. Data was taken in steps of 0.33 nm. Noting that the vertical scale can't be right. This occured after modifying the computer program to obtain 0.33 nm steps.

Chapter 4

Results and Discussion

4.1. Introduction:

The atmospheric sodium daytime abundance was calculated for Corvallis Oregon by direct absorption of sunlight by atmospheric sodium. The results obtained were found to be consistent with the results obtained by Partowmah (See Chapter 2 Sec.3.B). He calculated the abundance by calculating the equivalent width which is the integrated area under the curve of the absorption line [relative to the intensity of the incident radiation obtained using the parameters which describe the depth and width of the terrestrial absorption line(19)] due to absorption by terrestrial sodium versus the wavelength or frequency. Because of the weakness of the terrestrial sodium absorption, the computed equivalent width W measured in units per centimeter square was converted to an abundance value A using the following equation(18)

$$A = (m\ c^2\ /\pi\ e^2\ )\ (W/f) \quad cm^{-2}$$

$$= 1.13 \times 10^{12}\ \ (W/f) \quad cm^{-2}$$

where f is the oscillator strength (0.653 for D2).

An important point must be stated at this point, which is that the Fraunhofer absorption lines do form at the same solar atmospheric level as does the continuum. The strongest absorption lines originate in the upper photosphere, and the weaker ones originate in the lower photosphere (42). The chromospheric spectrum contains emission lines such as the hydrogen Balmer lines, and He lines. These lines fade with

height due to the rapid increase of temperature with height above the photosphere (See Figure 2.1), and also due the decrease of the gas density with height.

4.2. Calculating the abundance of atmospheric sodium

After careful check of many graphs of the solar spectrum, a fixed procedure has been taken to measure the depth of the sodium dip (absorption band due to the sodium D-lines) Δ log I, by averaging the values of the difference between the bottom of the dip and its top on both sides (See Figure 3.3), considering only the constant features of the line. Calculating the number of sodium atoms was done using equation (2.3.25), also taking advantage of the model discussed in section (2.3) assuming that the sodium layer lies between 80 to 105 km. Starting from the data which were taken around noon (Δ log I) and the next data (Δ log I') at later time, and assuming that $\Delta N = 0$ during this period (this assumption may cause some error, but around noon the number of sodium atoms doesn't change much). Now, it is easy to calculate the average density of atmospheric sodium N. The calculation is done for the next data and ΔN is calculated. The new sodium atom density is $N + \Delta N$. The abundance was calculated by multiplying the average density by the the thickness of the sodium layer (25 Km).

4.3. Results and discussion

The atmospheric sodium daytime abundance was measured by direct absorption of sunlight in the vicinity of the sodium D-lines. Measurements were taken in September and October, 1987(fourteen days

of measurements). The data show that the diurnal abundance of the atmospheric sodium increases until around noon, when it reaches maximum, then it starts to drop (See Figure 4.1,4.2,4.3). Also a day to day variation in the atmospheric sodium abundance is observed (See Figure 4.4, 4.5). The maximum value of the daily average abundance (13.189×10^9 atom/cm^2) was obtained on October 7,1987 with partially cloudy sky (See Figure 4.1). The minimum daily average abundance (0.865×10^9 atom/ cm^2) was obtained on October 19, 1987 with clear sky (See Figure 4.2). The total average abundance of atmospheric sodium on fourteen days of measurments is found to be 5.35×10^9 atom/ cm^2. Partowmah and Roestler(18) found that the maximum daily average abundance of atmospheric sodium to be 12×10^9 atoms cm^{-2} while our data showed it to be 13.189×10^9 atoms cm^{-2}. Also their data showed the minimum daily average abundance to be 2.9×10^9 atoms/ cm^2 while our data shwed it to be 0.865×10^9 atoms/ cm^2. Also their data showed a day-to-day variation of atmospheric sodium abundance and a daytime enhancement with maximum at noon.

The daytime enhancement may be explained as follows: The sodium atoms are formed on the expense of the sodium compounds until around noon, then the sodium compounds started to be formed on the expense of the sodium atoms.

At present, the day-to day variations in our data can't be explained, similar variations observed previously were attributed to a distinctly nonuniform pattern of mesospheric sodium concentration (18,43).

This experiment can be improved by improving the resolution power

of the spectrum analyzer (Its resolution power is 0.5 nm which is approximately the same as the wavelength separation of the sodium D lines.). By resolving the two D lines we can add the contribution of each line by making use of P(D2)/ P(D1) = 1.8 , and P(D1) + P(D2) = 1/ sec where P(D) is the probability of photon emission. Further development can be done by considering the the higher order terms in the model discussed in Chapter 2, Sec.4.

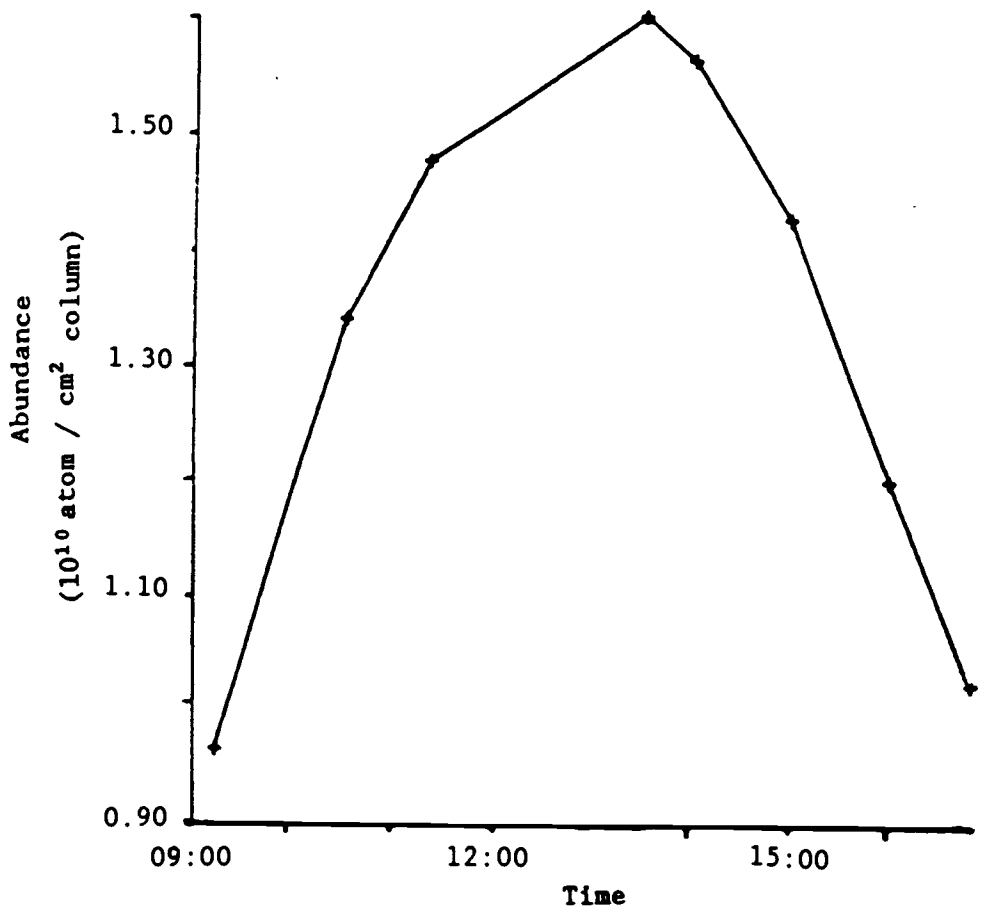

Figure 4.1 .The atmospheric sodium abundance on October 7, 1987. The sky was partially cloudy . The maximum average abundance was obtained on this day.

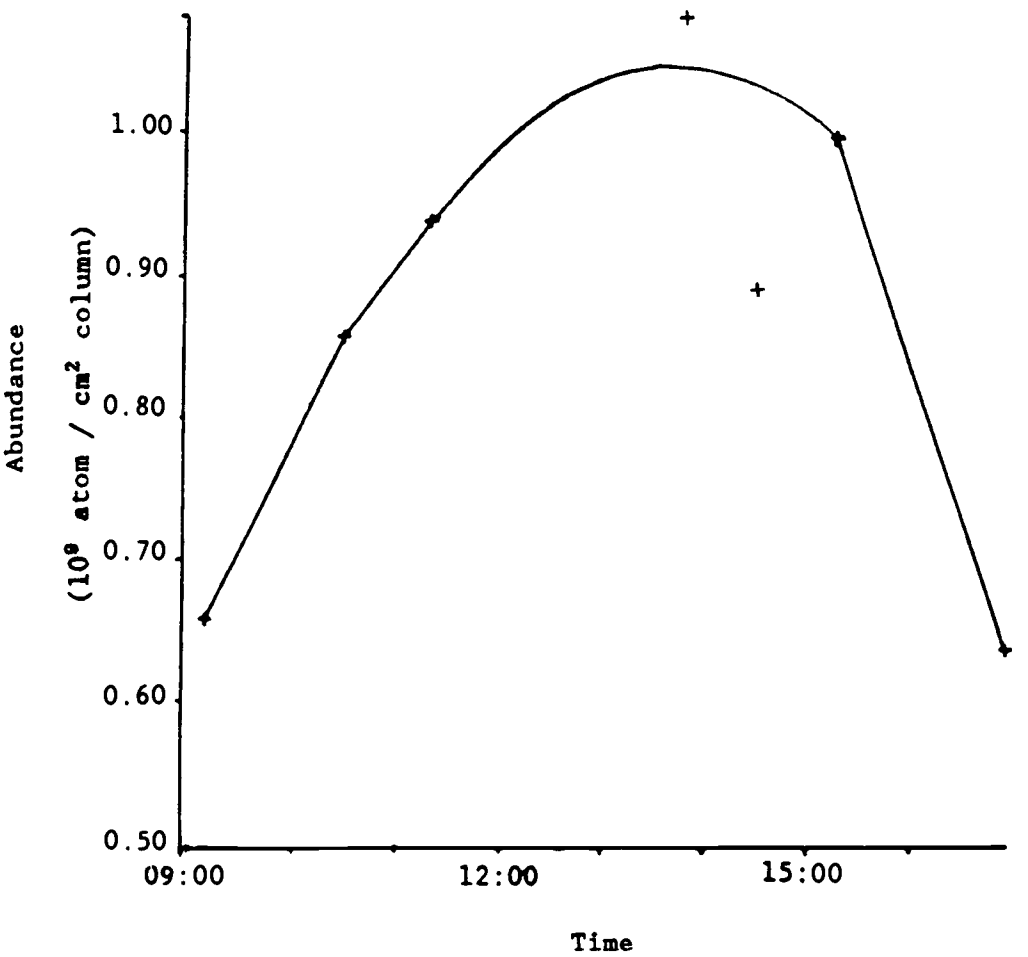

Figure 4.2 . The atmospheric sodium abundance on October 19, 1987. The weather conditions were good (clear sky). The minimum abundance was obtained on this day.

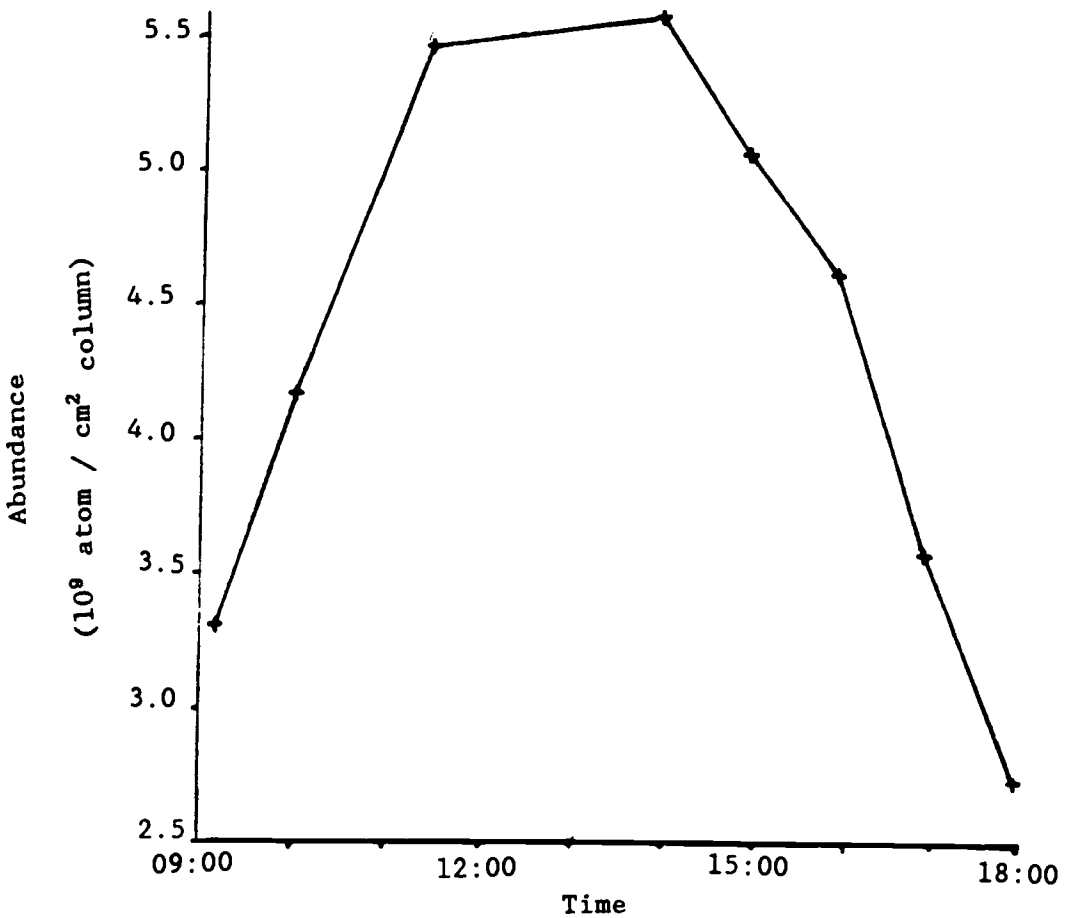

Figure 4.3. The atmospheric sodium abundance on September 17,1987. The sky was partially cloudy. Measurements were taken when the sun was uncovered with clouds.

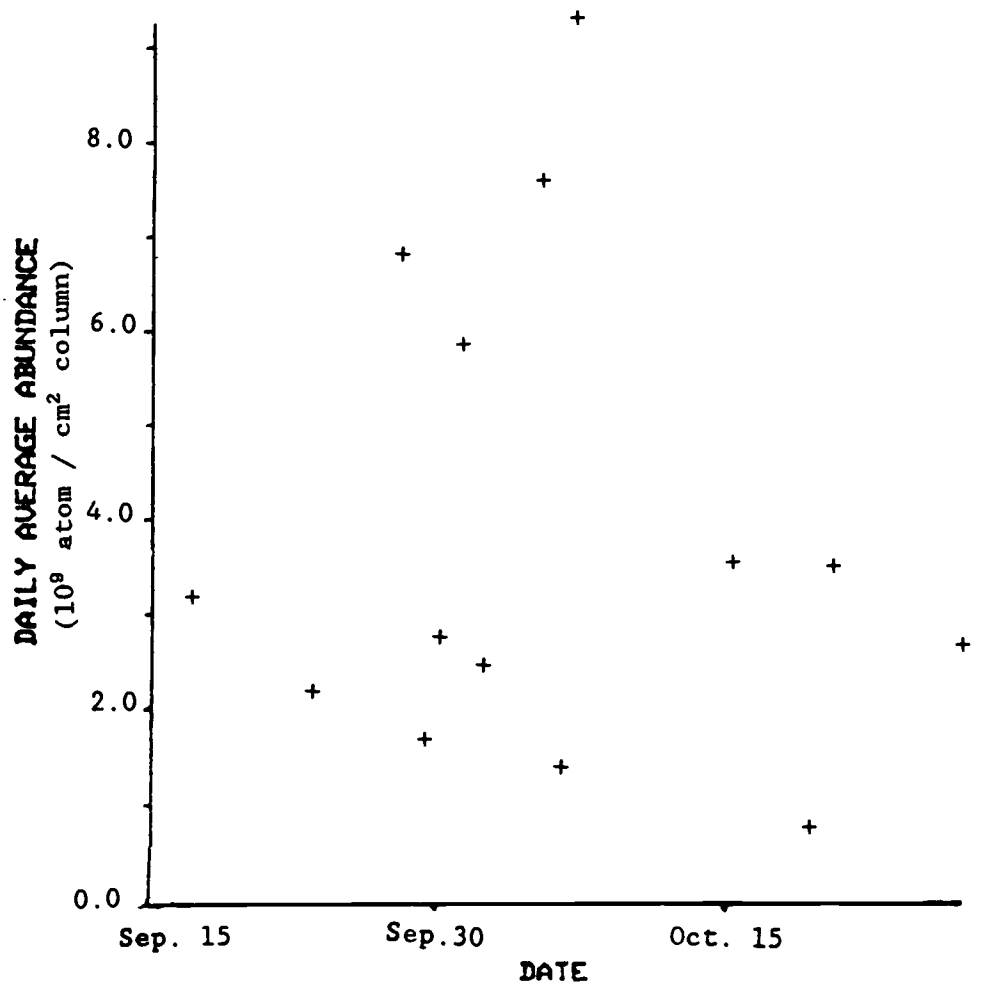

Figure 4.4. The atmospheric sodium daily average abundance on fourteen days of measurements. Measurements were taken in September and October 1987.

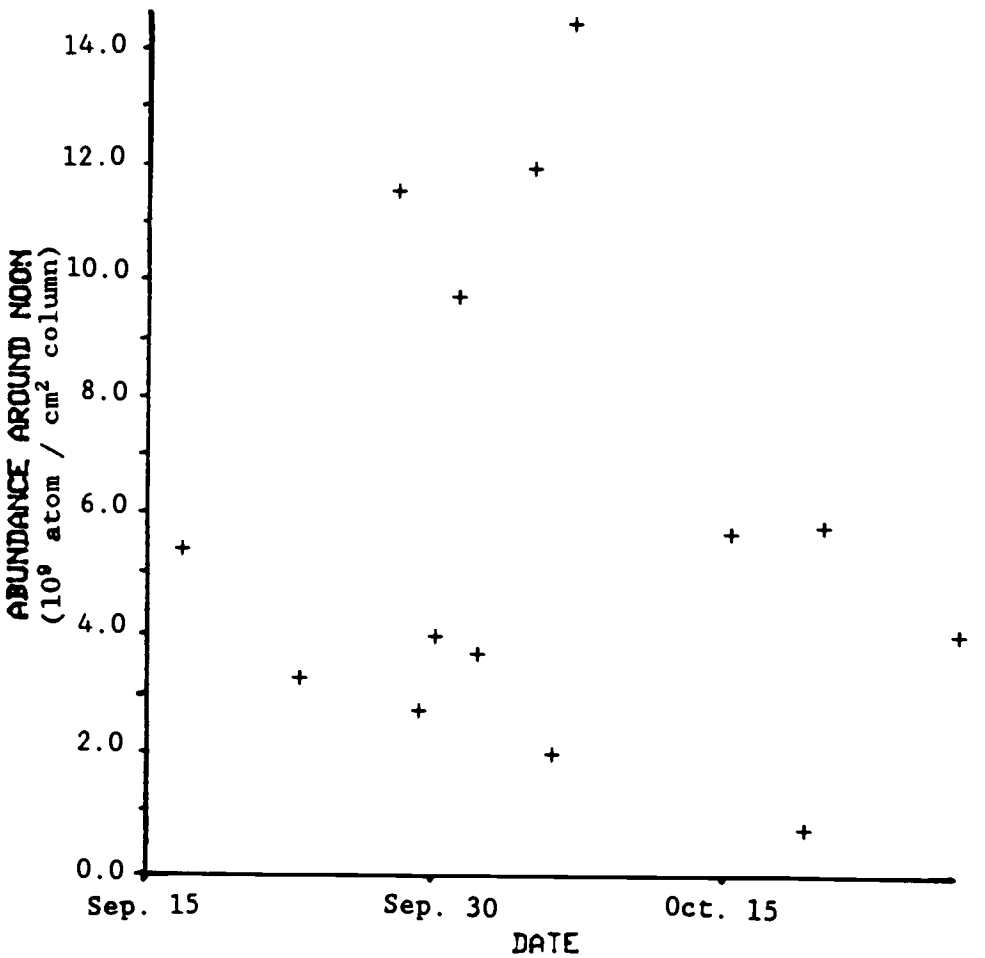

Figure 4.5. The atmospheric sodium abundance around noon on fourteen days of measurements. Measurements were taken in September and October 1988.

REFERENCES

1. S. K. Mitra, The Upper Atmosphere, (The Asiatic Society, Calcutta, 1952), pp. 538-548.

2. J. A. Ratcliffe, The Physics of the Upper Atmosphere, (Editted by J. A. Ratcliffe, Acadimic Press New York and London,1960).

3. L. Vegard, Relations enter les phenomenes Solaires et Geophysiques, (Center National de la Recherche Scientifique, Paris, 1947) , p. 254.

4. J. E. Blamont, in "The Airglow and the Aurora", (E.B.Armstrong and A. Dagarno, eds., Pergamon, London, 1956), p. 99.

5. M. L. Chanin, and J. P. Goutail, Diurnal variation of the sodium dayglow, J. Geophys. Res., 80, 2854, 1975.

6. D. M. Hunten, in "The Airglow and the Aurora", (E . B. Armstrong and A. Dalgarno, eds., Pergamon, London, 1956), p. 114.

7. D. M. Simonich ,B. R. Clemesha, and V. W. J. H. Kirchhoff, The measospheric sodium layer at 32 s: Nocturnal and seasonal variations, J. Geoph. Res. 84, 1543-1550, 1979.

8. V. Mitra, Origin and height distribution of the sodium in the earth's atmosphere, Ann. Geophys., 29, 341, 1973.

9. A. H. Woodcock, Salt nuclei in marine air as a function of altitude and wind force, J. Meteorol., 10, 362-371, 1953.

10. C. E. Jungge, O. Oldenberg, and J. T. Wasson, On the origin of the sodium present in the upper atmosphere, J. Geophys. Res. 67, 1027, 1962.

11. S. Chapman, Notes on atmospheric sodium, Astrophys. J., 90, 309-316, 1939.

12. F. S. Rowland, and Y. Makide, Upper atmospheric photolysis of NaOH, Geophys. Res. Lett., 9, 573-475, 1982.

13. D. M. Hunten, spectroscopic studies of the twilight airglow, Space Sci. Rev., 6, 493-576, 1967.

14. M. Gadsden, T. M. Donahue, and J. E. Blamont, on the measurement of sodium dayglow emission by means of a Zemman photometer, Geophys. Res., 71, 5047, 1966.

15. Clyde R. Burnett, Wayne E. Lammer, Walter T. Novak, and Victoria L. Sides, Absorption Measurements of upper atmospheric sodium at Boca Raton, Florida, 1967-1971, J. Geophys. Res., 77, 2934, 1972.

16. D. P. McNutt, and J. E. Mack, Telluric absorption, residual intensities and shifts in the Fraunhofer D lines, J. Geophys. Res., 68, 3419, 1963.

17. Clyde R. Burnet, Richard W. Lasher, Alan S. Mishkin, and Victoria L. Sides, Spectroscopic measurments of sodium dayglow: Absence of a large Diurnal variation, J. Geophys. Res. 80, 1837, 1975.

18. Mozaffer Partowmah and F. L. Roestler, Absorption studies of daytime sodium abundance, J. Geophys. Res., 82, 19, 1977.

19. V. W.J. H. Kirchhoff, Atmospheric sodium chemistry and diurnal variations, an up-date, J. Geophys. Res. 10, 721-724, 1983.

20. Donald R. Blake and F. Sherwood Rowland, Continuing worldwide increase in Tropospheric Methane, 1978 to 1987, Science, 239, 1069-1216, 1988.

21. E. M. Campell, Energy And The Atmosphere, A physical Chemical Approach, (Edited by John Wiker and sons LTD, Chichester, 1986, Second Edition), Chapter 4.

22. E. E. Ferguson, Sodium hydroxide ions in the stratosphere, Geophys. Res., 5, 1035-1038, 1978.

23. S. C. Liu, and G. C. Reid, Sodium and other minor constituents of meteorics origin in the atmosphere, Geophys. Res. Lett. 6, 283, 1979.

24. V. W. J. H. Kirchhoff and B. R. Clemesha, The atmospheric Neutral sodium layer 2. Diurnal variation, J. Geophys. Res. 88, 442-450, 1980.

25. E. Murad, and W. Swider, Chemistry of meteormetals in the stratosphere, Geophys. Res. Lett., 6, 929-932, 1979.

26. V. W. J. Kirchoff, B. R. Clemesha and D. M. Simonich, Seasonal variation of ozone in the Mesosphere, J. Geophys. Res., 86, 1463-1466, 1981.

27. V. W. J. H. Kirchhoff, B. R. Clemesha and D. M. Simonich, The atmospheric neutral sodium layer, 1. Recent Modeling compared to measurements, J. Geophys. Res. 86, A8, 6892-6898, 1981.

28. V. W. J. H. Kirchhoff, B.R.Clemesha, and D.M., Seasonal variation of ozone in the mesosphere, J. Geophys. Res., 86, 1463-1466, 1981.

29. B. R. Clemesha, V. W. J. Kirchhoff, D. M. Simonich, and P. P. Batista, Mesospheric winds from lidar observations of atmospheric

sodium, J. Geophys. Res., 86, 868-870, 1981.

30. L. Thomas, A. J. Gibson and S. K. Bahattacharrya, Lidar Observations of A horizontal Variation in The Atmospheric Sodium Layer, J. Atmos. Terr. Phys., 39, 1405-1409, 1977.

31. J. R. Rowlett, C. S. Gardner, E. S. Richter, and C. F. Sechrist, Jr., Lidar Observations of Wave-like Structure in The Atmospheric Sodium Layer, J. Geophys. Res., 84, 1543-1550, 1979.

32. V. W. J. H. Kirchhoff and B.R. Clemesha, Eddy diffusion coefficients in the lower thermosphere, 88, 5765-5768 ,1983.

33. John J. Lamb and Sidney W. Benson, Some kinetic and thermochemical aspects of sodium, J. Geophys. Res., 91, 8683-8689, 1986.

34. D. W. Hughes, Cosmic dust influx to the earth, Space Res., 15 ,531, 1975.

35. D. M. Hunten, R. P. Turco, and O. B. Toon, Smoke and dust particles of meteoric origin in the mesosphere and stratosphere, J. Atmos. Sci, 37, 1342, 1980.

36. J. E. Mack., D. P. McNutt, F. L. Roestler, and R. Chabbal, The pepsios purely interferometric high-resolution scanning spectrometer, 1, The pilot model, Appl. Opt., 2, 873, 1963.

37. G. S. Kent, B. R. Clemesha, and R. W. Wright, High altitude atmospheric scattering of light from laser beam, J. Atmos. Terr. Phys., 29, 169-181, 1967.

38. R. M. Goody, Atmospheric Radiation, I Theoretical basis, (Oxford at the Clarendon Press, 1964), pp. 97-100.

39. William J. Kaufman, Universe, (W. H. Freeman and Company New York, 1988, Second Edition), pp. 378-381.

40. A. Mitchell and M. Zemansky, Resonance Radiation and Excited Atoms, (Cambridge at the University Press, Cambridge, 1961), Ch.1 and 3.

41. S. Solimeno, B. Crosignans and P. Diporto, Guiding Diffraction and Confinment Of Optical Radiation, (Acadimic Press, inc., 1986), pp. 406-408.

42. Michael Zeilik and Elske V. P. Smith, Introductory Astronomy & Astrophysics, Second Edittion, (Editid by Sounders College Publishing, Philadelphia, 1986) pp. 184-190.

43. J. E. Blamont, and T. M. Donahue, The dayglow of the sodium D lines, J. Geophys. Res., 66, 1407, 1961.

44. J.R.Waldram, The Theory of Thermodynamics, (Cambridge University Press, Cambridge, 1985), pp. 50-51.

APPENDIX

APPENDIX

Doppler broadening line shape:

The shape of a spectral line depends mainly on the type or types of broadening . In the case of Doppler broadening where the molecules suffer random thermal motion we may take

$$K(v) = I_v \quad f(v-v_0)$$

where

$$\int_{-\infty}^{\infty} f(v-v_0) \quad d(v-v_0) = 1 \qquad (1)$$

v_0 is the frequency at the center of the line , and I_v is the intensity of the line, and $f(v-v_0)$ is the shape factor.

In Doppler broadening the absorping or emitting molecules have thermal velocity component $U \ll C$ and the Doppler shift can be written as

$$v = U\, v_0 \,/\, C \qquad (2)$$

If a stationary molecule has $f'(v,v_0)$ then $f(v,v_0)$ can be written as $f'[v-v_0 - (U/C)\, v_0]$. If the probability that the velocity component lies between U and U + d U is P(U) dU,then the shape factor due to all Doppler-shifted components is

$$f(v-v_0) = \int P(U)\, f(v-v_0 - U\, v_0/C)\, dU \qquad (3)$$

In the case of thermodynamic equilibrium P(U) is given by the Maxwell's one-component velocity distribution(44)

$$P(U) = (m / 2\ k\ T)^{1/2} \exp (- m\, U^{1/2} /2\ k\ T) \qquad (4)$$

where m is the mass of the molecule, k is Boltzman constant , and T is the absolute temperature. Since P(U) is Gaussian, then

$\Delta U = (2\ k\ T/\ m)^{1/2}$, and the width of f can be interpreted from

equation (2) as the effective velocity dispertion $\Delta U = \alpha C / v_0$. The value of the integral in equation (3) is governed by the the non-dimentional parameter

$$d = 2 \alpha / \{(v_0/C)(2 k T / m)^{1/2}\}$$

If $d \ll 1$, then f(U) is a narrow function compared to P(U). In the limit f(U) can be treated as a delta function, then simple integration over the delta function leads to

$$f(v-v_0) = (1/\alpha_D \sqrt{\pi}) \exp \{-(v-v_0)^{1/2}/\alpha_D^2\} \qquad (5)$$

where $\alpha_D = v_0/C (2 k T / m)^{1/2}$ is the Doppler width of the line.